Transient Buoyant Flows of a Stratified Fluid in a Vertical Channel

Jun Sang Park*
Department of Mechanical Engineering, Halla University

A theoretical analysis is performed to describe the qualitative behavior of transient buoyant flows in a vertical channel. Consideration is given to the case of a fluid with a pre-existing stratification. The fluid motion is generated by giving impulsive anti-symmetric step-changes in temperature at the vertical left and right sidewalls. The qualitative character of the flow is shown to be classified in the Rayleigh number (Ra)-Prandtl number (σ) diagram. The transitory approach to the steady state can be monotonic or oscillatory, depending on $(\sigma-1)^2\pi^4 \gtrless 4\sigma R_a$. The prominent characteristics of time-dependent flow are discussed for large R_a. The profiles of temperature and velocity in the transient phase are depicted, which disclose distinctive time scales of motion. The transient process is shown to be sensitive to the Prandtl number. The detailed evolutions of flow and temperature fields are illustrated for large R_a.

Key Words : Brunt-Vaisala Frequency, Stratified Fluid, Transient Bouyant Flow, Prandtl Number

Nomenclature

D : Horizontal length scale of the cavity
g : Acceleration of gravity
H : Vertical length scale of the cavity
R_a : Rayleigh number$[\equiv \alpha\beta T_0 D^4/\nu\chi]$
T : Temperature
T_0 : Basic temperature at $x=0$ and $z=0$.
u : Velocity component in the x-direction
w : Velocity component in the z-direction
x : Horizontal coordinate
z : Vertical coordinate
α : Coefficient of thermometric expansion
β : Coefficient of basic stratification in the vertical direction
δ : Thermal perturbation at vertical walls
χ : Thermal diffusivity
ν : Kinematic viscosity
σ : Prandtl number$[\equiv \nu/\chi]$
Ψ : Stream function

Subscripts

s : Steady part of the solution
u : Unsteady part of the solution

* **E-mail** : jspark@hit.halla.ac.kr
TEL : +82-33-760-1219; **FAX** : +82-33-760-1211
Assistant professor, Department of Mechanical Engineering, Halla University, San66, HeungUp, WonJu, Kangwon-do 220-712, Korea.(Manuscript **Received** August 3, 2000; **Revised** February 15, 2001)

1. Introduction

Natural convection in a rectangular cavity, whose two vertical walls are at different temperatures, has been extensively studied. The steady-state features in classical treatises (see, e. g., Batchelor, 1954; Elder, 1965; Gill, 1966) are characterized by three major nondimensional parameters, i. e., the system Rayleigh number R_a, the Prandtl number σ, and the container aspect ratio A_r. A particular attention has been focused on the case when there exists a prevailing vertical stratification, in addition to a temperature contrast in the horizontal direction which is applied between the two vertical sidewalls. This problem, in the steady state, was tackled by theoretical endeavors and exact steady solutions of the Boussinesq equation in an infinite vertical layer were secured (e.g., Gill, 1966; Elder, 1965; Bergholz, 1978). By examining the asymptotic structure of the base flow for large R_a, it is shown

that the mass flux is carried by the boundary layer of thickness $O(R_a^{-1/4})$ on the vertical wall. This type of boundary layer has been termed the buoyancy layer, and the dynamical significance of this layer has been asserted in a wide variety of strongly stratified fluid systems (e.g., Veronis, 1966; Barcilon & Pedlosky, 1966).

Although many investigations on natural convection in an enclosure have been concerned with steady-state situations, time-dependent flows of buoyant convection in a cavity have received far less attention (e. g., Hyun, 1994; Ravi et al., 1994; Janssen and Henkes, 1995; Schopf and Patterson, 1995; Park and Hyun, 1998). As observed by Jischke and Doty (1975), this scarcity does not imply that the time-dependent processes are in any way less important. Rather, this is reflective of the formidable difficulties involved in dealing with time-dependent convection problems in general. Recently, Park and Hyun (1998) tackled a transient buoyancy layer, in which they utilized an eigenfunction expansion method.

In this paper, a straightforward analysis along Park and Hyun (1998) is made of a comprehensive analysis for a transient motion of stratified fluid, which is generated by impulsive anti-symmetric step-changes of temperature at the left and right walls. As a result, a complete formal solution is sought to the governing unsteady equations of motion for the buoyant motion on an infinite vertical wall and also details of physical interpretation will be described. The criterion will be given for oscillatory or nonoscillatory approach to the steady state. These two modes in the transient process, i.e., one represents a monotonic approach and the other an oscillatory approach to the steady state, are shown to be accomplished by competing mechanism of radially thermal diffusion and vertical advection terms. The related $(R_a\text{-}\sigma)$ diagram for these two modes is ascertained.

2. The Flow Model

An incompressible, Boussinesq fluid of kinematic viscosity ν, thermal diffusivity $\varkappa$ and coefficient of thermometric expansion α, is contained in an infinite vertical channel of width 2D, in which the cartesian coordinates (x, z) and velocity vector $\vec{V}=(u, w)$ are adopted as shown in Fig. 1.

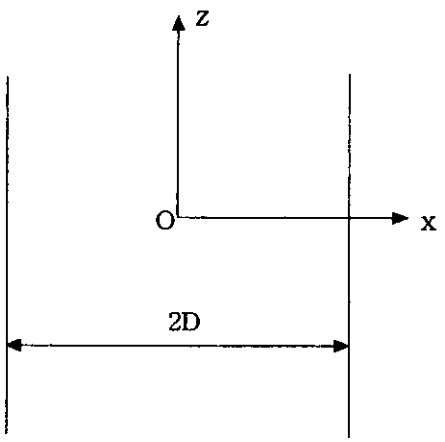

Fig. 1 Geometry of the problem

The fluid is motionless at the initial state ($t=0$), i.e., $u=w=0$, and the fluid is assumed to be in the state of a vertically-linear stable stratification, i.e.,

$$T=T_0(1+\beta z),$$

in which T_0 refers to the reference temperature.

The fluid motion is initiated by the fact that, at the initial instant $t=0$, the temperature on the right (left) vertical sidewall is abruptly increased (decreased) uniformly by ΔT. In this paper, the investigation is focused on the subsequent transient adjustment process leading to the steady-state equilibrium.

The nondimensional quantities, denoted by a prime , are as follows:

$$(x, z)=(x'D, z'D),\ t=t'\frac{D^2}{\varkappa},$$
$$\vec{V}=(u', w')=(u, w)/(\varkappa/D),$$
$$T'=[T-T_0(1+\beta z)]/(\beta T_0 D),$$
$$p'=\left(\frac{p}{\rho_0}\right)\frac{D^2}{\nu\varkappa}$$

The governing time-dependent equations, in the dimensionless form, are well established [after dropping the prime from the nondimensional quantities]:

$$\nabla\cdot\vec{V}=0, \tag{1}$$

$$\frac{1}{\sigma}\left(\frac{\partial \vec{V}}{\partial t}+\vec{V}\cdot\nabla\vec{V}\right)=-\nabla p+R_a T\vec{k}+\nabla^2\vec{V}, \quad (2)$$

$$\frac{\partial T}{\partial t}+\vec{V}\cdot\nabla T+w=\nabla^2 T \quad (3)$$

In the above, the principal dimensionless parameters emerge:
$\sigma\equiv\nu/\kappa$, the Prandtl number and $R_a\equiv\frac{\alpha g\beta T_0 D^4}{\nu\kappa}$, the system Rayleigh number.
Note that the temperature scale in the definition of Ra in the present study is $\beta T_0 D$, which indicates the vertical temperature difference in the initial-state stratification.

The initial conditions are $u=w=T=0$ at $t\leq 0$, (4)

and the boundary conditions are:
at the vertical walls $[x=\pm 1]$, $u=w=0$ and $T=\pm\delta$, $[\delta\equiv\Delta T/(\beta T_0 D)]$ (5)
Notice that, in the present study, the strength of the thermal forcing at the vertical walls is denoted by δ.

3. Transient Buoyant Flows in an Infinite Vertical Channel

Present problem setting gives a solution for z-independent flow, i.e., uniform variables along the vertical direction but it can be considered as an interior solution of finite cavity problem. If the cavity aspect ratio($A_r\equiv$height/width), or the system Rayleigh number is very large, the fluid in the bulk of the interior region does not feel the direct influence of the presence of the horizontal walls. The horizontal flows are confined to the horizontal boundary layers of thickness $O(A_r^{-1})$ or $O(R_a^{-1/8})$ on the horizontal endwalls (Jischke & Doty, 1975; Sakurai & Matsuda, 1972).

In the present development, the physical variables are functions of x and t. The problem is then reduced to describing buoyant fluid motions between two infinite vertical walls at different temperatures. By employing the streamfunction Ψ, which is defined such that $(u, w)=\left(-\frac{\partial\Psi}{\partial z}, \frac{\partial\Psi}{\partial x}\right)$, the governing equations are simplified to

$$\frac{1}{\sigma}\frac{\partial}{\partial t}\frac{\partial^2\Psi}{\partial x^2}=R_a\frac{\partial T}{\partial x}+\frac{\partial^4\Psi}{\partial x^4}, \quad (6)$$

and

$$\frac{\partial T}{\partial t}+\frac{\partial\Psi}{\partial x}=\frac{\partial^2 T}{\partial x^2} \quad (7)$$

The initial and boundary conditions can be rewritten as

$$\Psi(x, t=0)=0 \text{ and } T(x, t=0)=0;$$
$$\Psi(x=\pm 1, t)=0, \frac{\partial\Psi(x=\pm 1, t)}{\partial x}=0 \text{ and}$$
$$T(x=\pm 1, t)=\pm\delta H(t),$$

where $H(t)$ denotes the Heaviside step function.

The solution to the above equations is split into the steady and transient parts :

$$\Psi(x, t)=\Psi_s(x)+\Psi_u(x, t)$$

and

$$T(x, t)=T_s(x)+T_u(x, t),$$

in which subscripts s and u indicate respectively the steady and transient parts.

As remarked earlier, the steady solution satisfies the no-slip velocity conditions as well as the differential-temperature conditions at the two vertical walls. This exact solution is well documented (e.g., Batchelor, 1954; Gill, 1966; Bergholz, 1978):

$$T_s(x)=\frac{1}{2}\delta\left(\frac{\sinh(\lambda_1 x)}{\sinh(\lambda_1)}+\frac{\sinh(\lambda_2 x)}{\sinh(\lambda_2)}\right), \quad (8)$$

and

$$\Psi_s(x)=\frac{\delta}{2}\left(\frac{\lambda_1\cosh(\lambda_1 x)}{\sinh(\lambda_1)}+\frac{\lambda_2\cosh(\lambda_2 x)}{\sinh(\lambda_2)}\right), \quad (9)$$

in which $\lambda_1=\left(\frac{R_a}{4}\right)^{\frac{1}{4}}\cdot(1+i)$ and

$$\lambda_2=\left(\frac{R_a}{4}\right)^{\frac{1}{4}}\cdot(-1+i),\ i^2\equiv -1.$$

Obviously, in the limit $R_a\ll 1$, $T_s(x)\sim\delta\cdot x$ and $w_s\sim\delta\frac{R_a}{6}(x-x^3)$, which indicates a conduction-dominant regime.

In the opposite limit $R_a\gg 1$, the well-known result is recovered (Bergholz, 1978):

$$T_s\sim\delta\frac{|x|}{x}\exp(R(|x|-1))\cdot\cos(R(|x|-1))$$

and

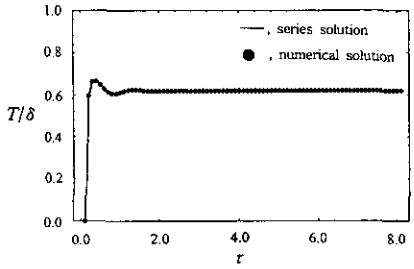

(a)

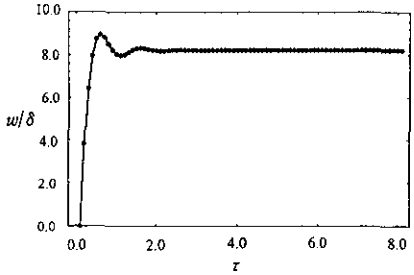

(b)

Fig. 2 Time history of : (A) temperature, T and (B) vertical velocity, w. $x=0.9$, $R_a=10^3$ and $\sigma=1.0$ The abscissa denotes the timescale as $\tau\equiv t\cdot R_a^{1/2}$

$$w_s\sim-\delta\cdot R\cdot\frac{|x|}{x}\exp(R|x|-1))\cdot\sin(R|x|-1))$$

where $R\equiv(R_a/4)^{1/4}$.

Now, the task is directed to the transient solution. The governing equation can be rewritten as

$$\frac{1}{\sigma}\frac{\partial^2 T_u}{\partial t^2}-\left(1+\frac{1}{\sigma}\right)\frac{\partial}{\partial t}\frac{\partial^2 T_u}{\partial x^2}+\frac{\partial^4 T_u}{\partial x^4}+R_a T_u=0, \tag{10}$$

with the boundary condition $T_u(x=\pm1,\ 0)=0$. The solution is sought in the form

$$T_u(x,\ t)=\sum_{n=0}^{\infty}T_n(x,\ t)\ \text{and}$$
$$w_u(x,\ t)=\sum_{n=0}^{\infty}w_n(x,\ t) \tag{11}$$

Substituting the expression $T_u(x,\ t)=\exp(a_n t)\cdot\sin(n\pi x)$ into Eq. (10), and after re-arranging, the eigenvalues a_n's are obtained:

$$a_{n1,2}=-\frac{(\sigma+1)(n\pi)^2}{2}\pm\frac{\sqrt{(\sigma-1)^2(n\pi)^4-4\sigma R_a}}{2} \tag{12}$$

Note that $a_{n1,2}$ are real only when $(\sigma-1)^2\pi^4>4\sigma R_a$.

The corresponding eigenfunction w_n and T_n can be rewritten as

$$w_n(x,\ t)=\frac{\partial\Psi_u}{\partial x}$$
$$=(C_{n1}\exp(a_{n1}t)+C_{n2}\exp(a_{n2}t))\cdot\sin(n\pi x), \tag{13a}$$

and, from Eq. (6),

$$T_n(x,\ t)=\left[C_{n1}\frac{(a_{n1}+\sigma(n\pi)^2)}{\sigma R_a}\exp(a_{n1}t)\right.$$
$$\left.+C_{n2}\frac{(a_{n2}+\sigma(n\pi)^2)}{\sigma R_a}\exp(a_{n2}t)\right]\cdot\sin(n\pi x) \tag{13b}$$

The complex-valued constants C_{n1} and C_{n2} are determined by making use of the initial-state fields that $T(x,\ 0)=T_s(x)+T_u(x,\ 0)=0$, $\partial T(x,\ 0)/\partial t=\partial\{T_s(x)+T_u(x,\ 0)\}/\partial t=0$ in the region $-1<x<1$. These considerations yield

$$C_{n1}=\frac{a_{n2}}{a_{n1}-a_{n2}}\int_{-1}^{1}w_s(x)\cdot\sin(n\pi x)dx$$

and

$$C_{n2}=\frac{-a_{n1}}{a_{n1}-a_{n2}}\int_{-1}^{1}w_s(x)\cdot\sin(n\pi x)dx$$

Consequently, the complete formal solution is given as

$$T(x,\ t)=T_s(x)+T_u(x,\ t)$$
$$=\frac{1}{2}\delta\left(\frac{\sinh(\lambda_1 x)}{\sinh(\gamma_1)}+\frac{\sinh(\lambda_2 x)}{\sinh(\lambda_2)}\right)$$
$$+\sum_{n=1}^{\infty}\left[\frac{\sigma R_a C_{n1}}{a_{n1}+\sigma(n)\pi^2}\exp(a_{n1}t)\right.$$
$$\left.+\frac{\sigma R_a C_{n2}}{a_{n2}+\sigma(n)\pi^2}\exp(a_{n2}t)\right]\cdot\sin(n\pi x), \tag{14a}$$

and

$$w(x,\ t)=w_s(x)+w_u(x,\ t)$$
$$=\frac{\delta}{2}\left(\frac{\lambda_1^2\sinh(\lambda_1 x)}{\sinh(\lambda_1)}+\frac{\lambda_2^2\sinh(\lambda_2 x)}{\sinh(\lambda_2)}\right)$$
$$+\sum_{n=1}^{\infty}(C_{n1}\exp(a_{n1}t)+C_{n2}\exp(a_{n2}t))$$
$$\cdot\sin(nx)\pi \tag{14b}$$

The evolutionary process of the temperature field in the buoyancy layer is, in general, governed by the Prandtl number σ and the Rayleigh number R_a. As shown in the above result, the strong influence of σ in the case of

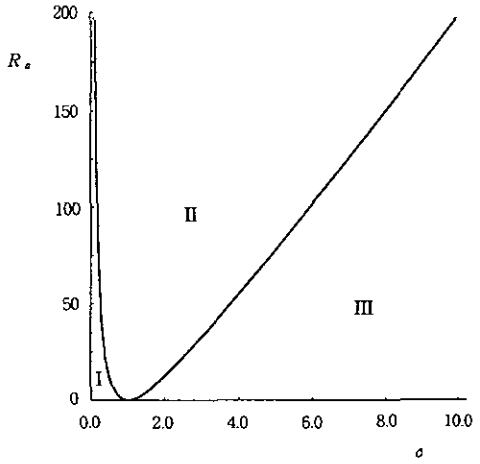

Fig. 3 Regime classifications in the $(R_a-\sigma)$ diagram. The boundary curve is given by $R_a=(\sigma-1)^2\pi^4/4\sigma$

transient process is in contrast to the case of steady state, in which the major features of flow are substantially independent of σ(Gill, 1966; Bergholz, 1978).

To check the accuracy of the series solutions (14a) and (14b), numerical solutions of Eqs. (6) and (7), which were obtained by utilizing finite difference scheme of a backward difference in time and a central difference in space on a uniform grid of 401 points, are compared with the series solutions. As shown in Fig. 2, the agreement between the series and numerical solutions is very good and the series solutions were obtained by adding the terms up to the 50th term. In Fig. 2, the time histories of temperature and vertical velocity are plotted at $x=0.9$, located within the vertical boundary layer, and the nondimensional parameters of flow system are $R_a=10^3$ and $\sigma=1.0$.

As can be readily seen in Eq. (12), the general temporal character of the temperature field is monotonic if $(\sigma-1)^2\pi^4\geq 4\sigma R_a$, and oscillatory if $(\sigma-1)^2\pi^4<4\sigma R_a$. The demarcation line in the $\sigma-R_a$ diagram is illustrated in Fig. 3. For a given value of Ra in regimes I and III, the transient process is non-oscillatory. Qualitatively, in regime I [III], the Prandtl number is generally very low [high]. Crudely speaking, this implies that the overall process is conduction

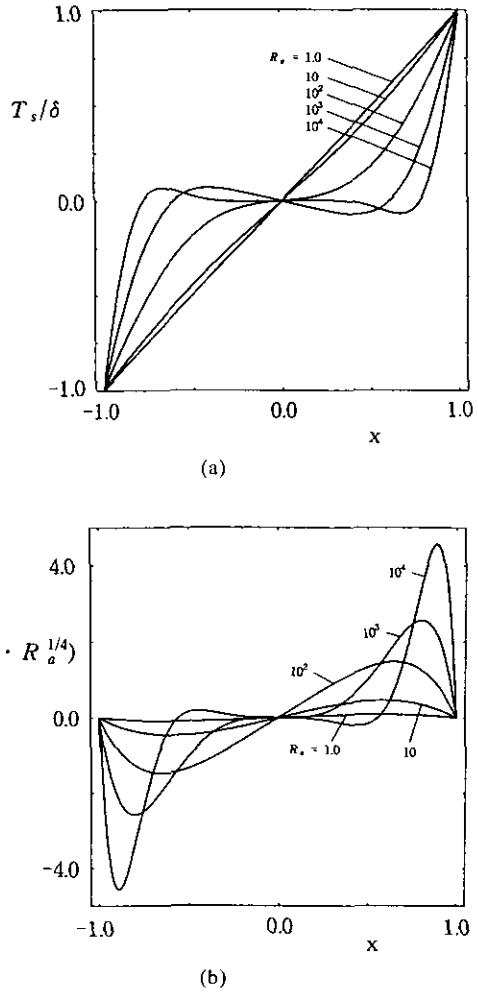

Fig. 4 Profiles of : (a) temperature ; (b) vertical velocity in the steady state. $\sigma=1$

[convection] - dominant, which precludes an overwhelming influence of one particular mode of heat transfer over the other. In regime II, the Prandtl number is intermediate. Again, this suggests that the conduction effect in the horizontal direction and the vertically-directed convection effect are comparable and competing. These produce an environment which is prone to oscillatory behavior. As is evident in Fig. 3, the range of σ for which oscillation is possible is enlarged as R_a increases. In particular, Eq. (12) indicates that, if $\sigma=1$, the transient process is oscillatory. For this case, the frequency of oscillation is precisely the Brunt-Vaisala fre-

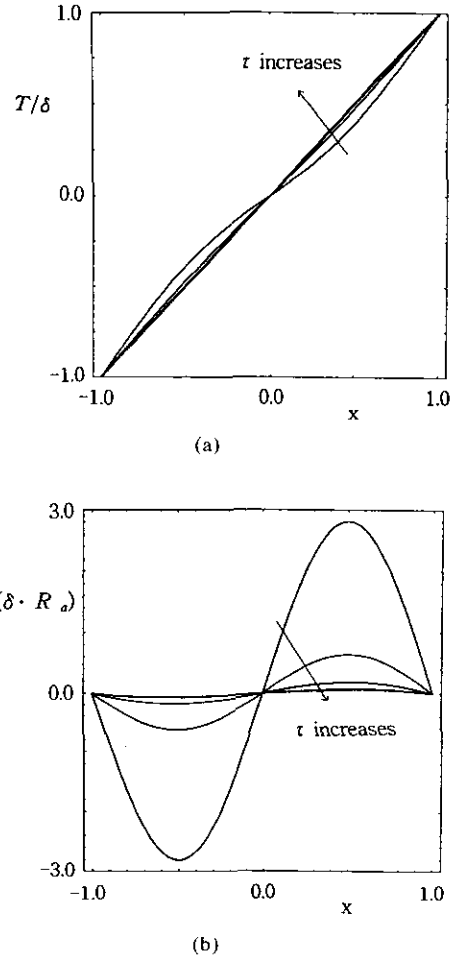

Fig. 5 Profiles of : (a) temperature; (b) vertical velocity in the transient state. $\sigma=1.0$ and $R_a=0.1$. Time is scaled as $\tau\equiv t\cdot R_a^{1/2}$. τ for the curves are 0.1, 0.15, 0.2, 0.3, ∞

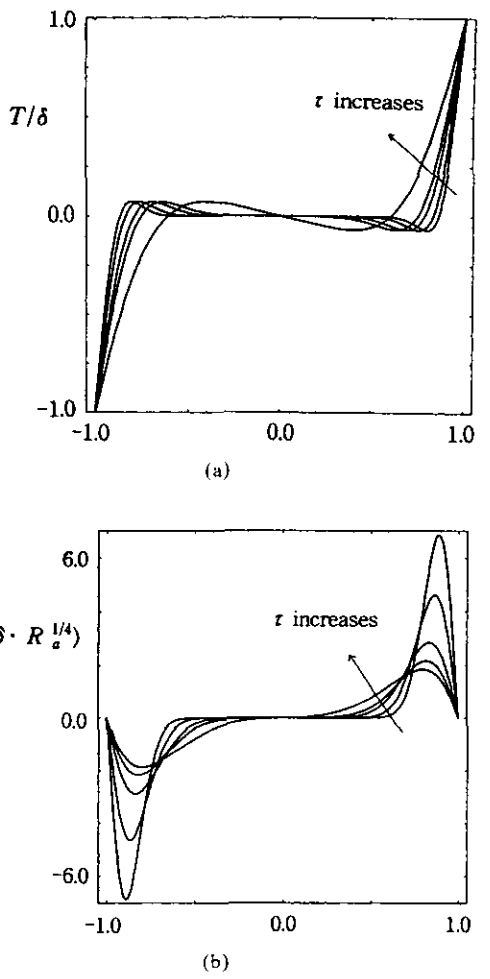

Fig. 6 Same as in Fig. 4, except for $\sigma=1.0$ and $R_a=10^3$. Time is scaled as $\tau\equiv t\cdot R_a^{1/2}$. τ for the curves are 0.2, 0.3, 0.5, 0.7, ∞

quency of the system, $R_a^{1/2}$.

Exemplary flow details are now presented to illustrate the principal aspects of the buoyancy layer. First, Fig. 4 reiterates the well-known steady-state features. When R_a is small, conduction is the primary mode of heat transfer. In this case, the temperature profile is linear, and the velocity is very small throughtout the entire fluid domain. As R_a increases, the effect of convection strengthens. At large R_a, the flow pattern bears the distinctive boundary layer-type features. In this limit, the spatial variations in temperature and velocity profiles are concentrated in the boundary layers near the wall. In the bulk of the interior, both the temperature and velocity gradients are small. It is worth mentioning that, at large R_a, there is a weak overshooting of the velocity and temperature profiles in the vicinity of the edge of the boundary layer.

The transient features are now scrutinized. The conduction-dominant behavior for small R_a is illustrated in Fig. 5(a). The spatial variation of temperature is largely linear, and the temporal evolution is characterized by the diffusive time scale. The corresponding velocity profile for small R_a is shown in Fig. 5(b), which demonstrates the expected features in the conduction-controlled regime.

Figure 6 exhibits the results for large R_a. Im-

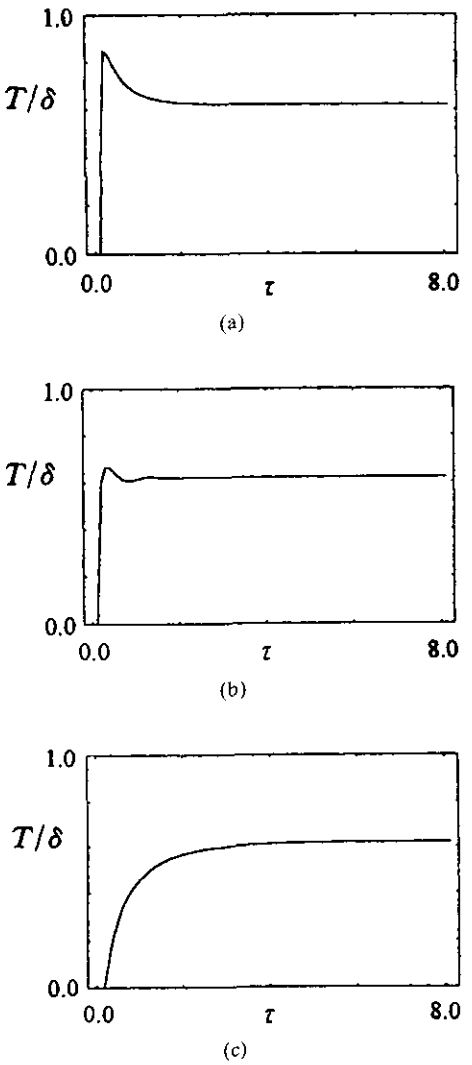

Fig. 7 Time history of temperature at $x=0.9$, $R_a=10^3$. The abscissa denotes the time scaled as $\tau \equiv t/(0.04\times 2\pi \times R_a^{-1/2}\times \sigma^{-1/2})$. The Prandtl number σ is : (a), 0.01(regime I); (b), 1.0 (regime II); (c), 300 (regime III)

mediately after the impulsive step-change of temperature at the wall, the heat flux in the vicinity of the wall is comparatively large. This generates buoyancy of relatively large magnitude, which induces vertical motion of appreciable strength in the boundary layer. When R_a is large, the overall heat balance in the boundary layer is maintained between the horizontal heat conduction through the wall and the vertical heat convection by the buoyancy-induced motion. Therefore, in the bulk of the interior, the fluid is largely motionless, and the initial temperature field remains substantially unaffected. As time elapses, the velocity and temperature profiles in the boundary layer broaden to approach the steady-state patterns shown earlier. It is also noticed that, until intermediate times, the velocities in the region of the boundary-layer edge exhibit overshoots.

Representative time-histories of transient temperature and velocity at $x=0.9$ are plotted in Fig. 7 for the three afore-stated regions I, II and III, respectively. In region I[Fig. 7(a)], temperature rises rapidly at very small times, and then, it decreases monotonically to the steady state. In region II[Fig. 7(b)], the temperature behavior exhibits an oscillatory approach, and in region III [Fig. 7(c)], the temperature increases monotonically.

The above transient features can also be explained from Eq. (7), which can be rewritten as follows:

$$\frac{\partial T}{\partial t}=-w+\frac{\partial^2 T}{\partial x^2}$$

The first term of the right-hand-side of the above equation represents vertical convection, and the second term indicates thermal diffusion in the horizontal direction. At a given location, the vertical convection of $w>0$ implies cool-down by bringing the fluid upward from below, which is colder. On the other hand, for $\delta>0$, thermal diffusion from the wall raises the temperature in the boundary layer. As shown in the above equation, the transient features are determined by the above two opposing effects. In region I $[(\sigma-1)^2\pi^4>64\sigma R_a$ and $0<\sigma<1.0]$, at very small times, thermal diffusion from the wall is dominant, which causes the temperature to rise rapidly and to overshoot the steady state value at large-time limit. With the passage of time, since σ is low, the weakening of temperature gradients at this location is pronounced, in which the effect of vertical advection outweighs thermal diffusion. The temperature is lowered accordingly, and, as time elapses, the temperature tends smoothly to the large-time limit. In region II $[(\sigma-1)^2\pi^4<64\sigma R_a$ and $0<\sigma<\infty]$, these effects alternate for control

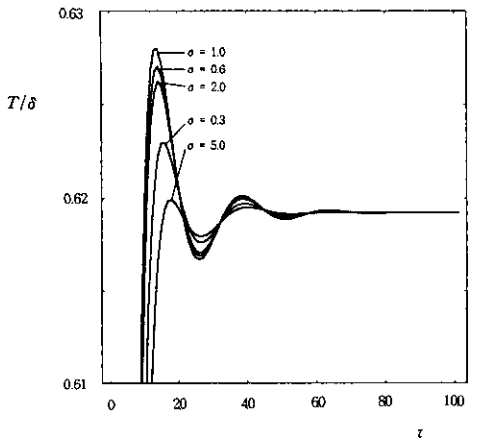

Fig. 8 Enlarged views of time-history of T at $x=0.9$ (regime II), $R_a=10^3$. The abscissa denotes the time scaled as $\tau \equiv t/(0.04\times 2\pi \times R_a^{-1/2}\times \sigma^{-1/2})$

of the boundary layer development, which results in oscillatory behavior. In region III $[(\sigma-1)^2\pi^4>64\sigma R_a$ and $1.0<\sigma<\infty]$, since σ is large, thermal diffusion proceeds at a slow rate. The effect of thermal diffusion is larger than that of vertical advection, and temperature rises monotonically with time.

The impact of σ on the oscillatory behavior in regime II is further scrutinized in Fig. 8. Evidently, the oscillatory character is most pronounced when $\sigma=1.0$. As is discernible in Eq. (12), when $\sigma=1.0$, the imaginary part of the eigenmode becomes $\pm iR_a^{1/2}$, regardless of the index n. This implies that the frequency of oscillation is the same for all the modes. However, as σ deviates from 1.0, the frequencies of oscillations differ for different eigenmodes. This type of dispersion reduces the amplitudes of oscillations, and the plots in Fig. 8 are consistent with the above reasoning.

4. Concluding Remarks

By eigenfunction expansion method, it has obtained the complete formal solution for the transient buoyant flows for an infinite vertical wall. It showed a strong dependence on σ during the transient phase of the buoyant motion, which is in contrast to the case of the steady-state layer. Both effects of Prandtl and Rayleigh numbers were described in detail with a comprehensive physical interpretation. It showed that the series solutions are in a good agreement with full-dressed numerical solutions. The transitory approach to the steady state is monotonic or oscillatory, depending on $(\sigma-1)^2\pi^4 \gtrless 4\sigma R_a$. In particular, if $\sigma=1$, the oscillation frequency is given by the Brunt-Vaisala frequency of the system. As R_a increases, transient oscillatory behavior is expected over a broader range of σ.

Acknowledgements

This work was supported by grant number 2000-2-30500-003-5 from the Basic Research Program of the Korea Science and Engineering Foundation.

References

Barcilon, V. and Pedlosky, J., 1966, "Linear Theory of Rotating Stratified Fluid Motions," *J. Fluid Mech.*, Vol. 29, pp. 1~16.

Batchelor, G.K., 1954, "Heat Transfer by Free Convection across a Closed Cavity between Vertical Boundaries at Different Temperatures," *Quart. Applied Math.*, Vol. 12, pp. 209~233.

Bergholz, R.F., 1978, "Instability of Steady Natural Convection in a Vertical Fluid Layer," *J. Fluid Mech.*, Vol. 84, pp. 743~768.

Elder, J.W., 1965, "Laminar Free Convection in a Vertical Slot," *J. Fluid Mech.*, Vol. 23, pp. 77~98.

Gill, A.E., 1966, "The Boundary Regime for Convection in a Rectangular Cavity," *J. Fluid Mech.*, Vol. 26, pp. 515~536.

Hyun, J.M., 1994, "Unsteady Buoyant Convection in an Enclosure, Advances in heat transfer," Vol. 24, pp. 277~320.

Janssen, R.J. A. and Henkes, R.A. W.M., 1995, "Influence of Prandtl Number on Instability Mechanism and Transition in a Differentially Heated Square Cavity," Vol. 290, pp. 319~344.

Jischke, M.C. and Doty, R.T., 1975, "Linearized Buoyant Motion in a Closed Container," *J. Fluid Mech.*, Vol. 71, pp. 729~754.

Park, J.S. and Hyun, J.M., 1998, "Transient Behavior of Vertical Buoyancy Layer in a Stratified Fluid," *Int. J. Heat & Mass Transfer*, Vol. 41, pp. 4393~4397.

Sakurai, T. and Matsuda, T., 1972, "A Temperature Adjustment Process in a Boussineaq Fluid via a Buoyancy-induced Meridional Circulation," *J. Fluid Mech.*, Vol. 54, pp. 417~421.

Schopf, W. and Patterson, J.C., 1995, "Natural Convection in a Side-Heated Cavity: Visualization of the Initial Flow Features," Vol. 295, pp. 357~379.

Ravi, M.R., Henkes, R.A. W.M. Henkes and Hoogendoorn, C.J., 1994, "On the High-Rayleigh-Number Structure of Steady Laminar Natural-Convection Flow in a Square Enclosure," Vol. 262, pp. 325~351.

Veronis, G., 1970, "The Analogy Between Ratating and Stratified Fluids," *Ann. Rev. Fluid Mechanics*, Vol. 2, pp. 37~67.